Journal of Nano Research, Volume 58, 2019, pp. 125-138
DOI:10.4028/www.scientific.net/JNanoR.58.125

New pH Correlations for Stainless Steel 316L, Alumina, and Copper(I) Oxide Nanofluids Fabricated at Controlled Sonication Temperatures

Naser Ali[1,2,a,*], Joao A. Teixeira[1,b], and Abdulmajid Addali[1,c]

[1]*Cranfield University, School of Aerospace, Transport and Manufacturing (SATM), Cranfield, England, MK430AL, UK*

[2]*Nanotechnology and Advanced Materials Program, Energy and Building Research Center, Kuwait Institute for Scientific Research, Safat 13109, Kuwait*

E-mail: [a]nmali@kisr.edu.kw, [a]naser.ali@cranfield.ac.uk, [b]j.a.amaral.teixeira@cranfield.ac.uk, [c]a.addali@cranfield.ac.uk

Keywords: Aluminium; Copper(I) oxide; Nanofluids; pH correlation; Stainless steel 316L.

Abstract. This research investigates the pH value of stainless steel (SS) 316L/ deionised water (DIW), alumina (Al_2O_3)/DIW, and copper(I) oxide (Cu_2O)/DIW nanofluids prepared using a two-step controlled sonication temperature approach of 10°C to 60°C. The nanoparticles volumetric concentration of each family of as-prepared nanofluid ranged from 0.1 to 1.0 vol%, using as-received nanopowders, of 18 – 80 nm average particles size. Furthermore, the pH measuring apparatus and the measurement procedure were validated by determining the pH of commercially supplied calibration fluids, of pH 4, 7, and 10. Following the validation, pH correlations were obtained from the experimental measurements of the 0.1, 0.5, and 1.0 vol% nanofluids in terms of varied sonication bath temperatures and volumetric concentrations. Those correlations were then combined into one robust pH_{nf} correlation and validated using the pH data of the 0.3 and 0.7 vol% nanofluids. The new proposed correlation was found to have a 2.18%, 0.92%, and 0.63%, average deviation from the experimental pH measurements of SS 316L, Al_2O_3, and Cu_2O nanofluids, respectively, with an overall prediction accuracy of ~ 92%.

Introduction

A new class of engineered fluids that rely on the dispersion of metals, metal oxides, allotropes of carbon, or a combination of any of these materials in the form of nanoparticles (NPs) of average diameter less than 100 nm and of low concentration, preferably < 1 vol%, in a non-carcinogenic basefluid (e.g. water, oil, kerosene, glycols etc.) were defined by Choi in 1995 as 'Nanofluids' [1-3]. This advance category of fluids have gained the interest of many researchers due to their distinctive properties compared to conventional fluids in the field of heat transfer enhancement, drug delivery, paint additives, magnetic sealing, ionic liquid synthesis, etc [4-11]. Although significant research findings on the thermophysical properties of different nanofluids and their applicability are available in the literature, there is still a need for better understanding of the fluid stability behaviour [12, 13]. To be more specific, the interaction between the NPs themselves and between the particles with the surrounding medium is still considered to be an area of exploration and of major concern. In general, nanofluids stability can be subclassified into dispersion stability, and kinetic stability [14]. Dispersion stability takes into account both the Van der Waals attraction force between the particles, and the electrostatic repulsion force caused by the electrical double layers on the particles surface, where clusters formation or agglomerations of particles are more likely to occur in a nanofluid when the attraction force is higher than the particle electrostatic repulsion force [15]. On the other hand, the kinetic stability describes the NPs dynamic Brownian motion in the basefluid, which causes particle sedimentation or phase-separation due to gravitational force [16]. The problem arising from the two aforementioned mechanisms is their negative impact on the long term stability of the suspensions if not appropriately dealt with, and hence can degrade the nanofluid thermophysical properties [17-19]. Basically, there are three main approaches to improve the stability of nanofluids: 1- sonicating the fluid, 2- adding surfactant, and 3- adjusting the pH value to optimize the zeta potential. Sonication, which is a physical method that depends on employing ultrasonic waves through the fluid, can be used to enhance the stability of the solution by rupturing the particles attractional force within the sediments [20]. Furthermore, using a surfactant of organic compounds that has hydrophilic head and hydrophobic tail group, has shown to be useful in increasing the stability of the aqueous solutions [21]. In addition, manipulating the pH value of nanofluids changes the NPs surface and can strongly improve the stability of the dispersed NPs [22, 23]. This is because the zeta potential, which is the potential difference between the layered fluid attached to the particles

and the dispersed particles surface, can be increased/decreased by changing the pH value and/or adding surfactant to the nanofluid. In principle, zeta potential values of nanofluids above +30 mV or below -30 mV are considered to be more stable due to the high repulsive force generated between the charged NPs [24-26]. Implementing one or more of the aforementioned techniques can result in obtaining a more homogeneous and better dispersed nanofluid.

Several studies were undertaken to illustrate the influence of the pH value on the nanofluids stability [27-39]. For example, Manjula et al. [40] examined the effect of pH value and surfactants on the suspension behaviour of alumina (Al_2O_3)/H_2O nanofluid via monitoring the formed sedimentations in the fluid. It was found that optimizing the pH value and adding surfactant to the nanofluid have resulted in maximising the stability of the nanosuspension. Witharana et al. [41] studied the aggregation and settling performance of 0.5 wt% (Al_2O_3)/H_2O nanofluid, of 46 nm particle diameter and water of pH of 6.3 and 7.8. Their results showed that the samples made of pH 6.3 were stable for more than 30 minutes, and that the nanofluids fabricated with a basefluid of pH 7.8 had a complete settling and particles separation after 30 min. Lee et al. [42] examined the stability and effective thermal conductivity of copper(II) oxide (CuO), of 25 nm average particles diameter, suspended in deionized water. Measurements of the formed agglomeration particles size, for the nanofluids of pH 3 to 11, have revealed that the attracted particles were mostly sized between 160 to 280 nm. It was concluded that the stability of the nanofluid was highly influenced by the pH value and the hydrodynamic size of the embedded particles. In addition, at a pH value of 11, the effective thermal conductivity has shown 11% enhancement over that of the basefluid. Song [43] studied the possibility of stabilising stainless steel (SS) 316L/ H_2O nanofluids, of 70 nm average particles size, with added surfactants of sodium dodecylbenzene sulfonate (SDBS) and sodium dodecyl sulfonate (SDS). In their experiment, the nanofluids investigated were adjusted to a pH value of 8.0, 9.0, 10.0, 11.0, and 12.6, before determining their durability and stability. Five approaches were used for their characterisation, namely: 1- absorbance measurement, 2- particle size distribution measurement, 3- sedimentation observation, 4- transmission electron microscope (TEM) observation, 5- zeta potential measurement. The long term stability analysis illustrated that the fabricated suspension of pH 11 maintained for 10 days, pH 10 maintained for 3 days, and those of less pH value have fully settled within one day. On the other hand, the nanofluid of pH 12.6 showed an excess amount of OH^- ions, which resulted in disturbing the electrostatic stability, causing the particles to rapidly settle.

Our review of the available literature quoted above shows that the pH value of nanofluids has a strong effect on its stability, and that the pH value of the suspension is influenced by its temperature and NPs concentration. The effect of a fluid pH was also reported to extend to the level of changing the wettability nature of the surface in contact to it [44, 45]. Given these facts, using an ultrasonic device for preparing nanofluids will lead to an increase in the fluid temperature and hence affect the resulting pH value of the nanofluid. This rise in temperature is limited by the surrounding atmospheric temperature of the site where the nanofluid is been prepared. This fact needs to be factored in when the commercial production of nanofluids in large scale is considered.

To the best of our knowledge, there is no existing empirical or theoretical relation that links the nanofluid controlled fabrication temperature and concentration to its pH value. Therefore, in this study, the pH value of SS 316L, copper(I) oxide (Cu_2O), and aluminium (Al) NPs dispersed in deionised water (DIW), was measured experimentally at range of controlled sonication bath temperatures and particle concentrations. An empirical correlation was then developed from the measured pH values, controlled fabrication temperatures, and particle concentrations of the prepared nanofluids and validated to help estimate the pH value of similar nanofluids robustly, within the same range of conditions. Such correlation is expected to be beneficial to nanofluids manufacturers and even researchers, where it can aid them in predicting the fluids pH value beforehand, so that a more convenient nanofluid with the desired stability can be achieved.

Experimental procedure

Materials. Portable pH meter calibration fluids of values 4, 7, and 10 were purchased from Metrohm USA Inc. A purity of 99.9% Al NPs and SS 316L NPs, of spherical particles shape and particles size between 40 to 60 nm and 60 to 80 nm, respectively, were purchased from SkySpring Nanomaterials. The chemical composition, as supplied by the manufacture, of the SS 316L NPS is shown in Table 1. A 99.86% super fine Cu_2O NPs, of 18 nm average particles size, were supplied by US Research Nanomaterials. A set of 40 mL, 27.5 mm outer diameter and 95 mm height, glass clear vials with screwed top were provided by SIGMA-ALDRICH. Deionised water, produced by an Elga PR030BPM1-US Purelab Prima 30 water purification system, was used as the basefluid for the nanofluids preparation after adjusting its pH value to 7.

Table 1. Stainless steel 316L chemical composition, wt% [46].

Elements	Cr	Ni	Mo	Si	Mn	S	C	P	Fe
wt%	16-18	10-14	2-3	0.75 max	2 max	0.03 max	0.03 max	0.045 max	balance

Characterization. Characterization tests were performed for the SS 316L, Al, and Cu_2O NPs through a 9 kW Rigaku SmartLab, Japan, X-ray diffraction (XRD) analyser and its software, SmartLab Guidance, using a CuKα X-ray source with a diffraction angle of 2θ and an incidence beam step of 0.2° to determine the Bragg's peaks of each element contained in the examined sample. The diffraction scanning angle range was from 20° to 80°, with a scanning rate of 1°/min. NPs densities were obtained in order to calculate the nanoparticle volumetric concentrations, which was required for the nanofluids fabrication. This was done by first measuring the samples weight, using an ae-ADAM PW 214 analytical balance of 0.0001 g readability and ±0.0002 g accuracy, then placing them in a HumiPyc trademark Model 1 gas pycnometer – volumetric analyser at an operational temperature of 25°C. The pH values of the DIW and fabricated nanofluids were measured from inside the vials, after placing them on a benchtop, by immersing the Hach PHC20101 Intellical pH measuring electrode connected to a HACH HQ40D portable pH meter, of accuracy ±0.002 pH, vertically to a depth of 5 cm then obtaining the reading for three times and averaging the values. The aforementioned procedure was done after calibrating the pH meter, before each conducted measurement and taking into account the temperature compensation, using the three as-received calibration fluids and the manufacturer instructions [47, 48]. Fig. 1 illustrates the experimental setup used for measuring the pH value of the nanofluid samples, which was also adopted for measuring the DIW pH value, at different temperature gradient.

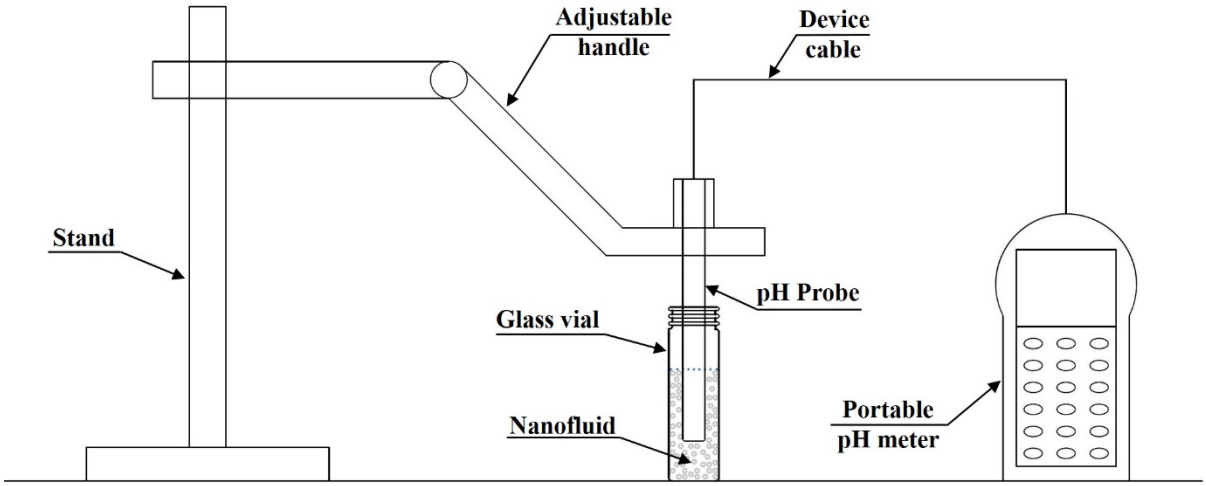

Fig. 1. Experimental setup used in measuring pH value of nanofluids samples.

Nanofluids preparation. Each nanofluid sample was prepared by placing the NPs first inside the vial then injecting 20 mL of DIW, using a disposable syringe, on top of the nanopowder after which the vial was sealed using the provided cap. The volume concentrations (φ) of NPs used were 0.1, 0.3, 0.5, 0.7, and 1.0 vol%, for each individual type of material. The vial containing the solution was then placed gently in a Soniclean company benchtop bath type ultrasonic vibrator, running at 100% power (43 kHz pulse) and filled with water to the recommended operating level by the manufacturer, for 4 hours to agitate the mixture. This kind of particles dispersion method is known as the two-step approach, which is a common procedure used for the production of nanofluids by many researchers [16, 33]. The sonicator bath temperature was then controlled, at a margin of ±1°C, for a temperature (T) that ranged from 10°C to 60°C, with an increment of 10°C, by gradually adding hot or cold water inside the ultrasonic bath and extracting the access water from the device via the attached ejection valve. This was done in order to characterise the variation in nanofluids pH (pH_{nf}) value at different points of temperature (e.g. pH value of nanofluid fabricated for 4 hours at fixed sonication bath temperature of 30°C with a margin of ±1°C). It should be pointed out that the lab temperature, where the experiments were performed, was 25°C and that surfactants or dispersing materials/chemicals were not used for the production of the nanofluids to avoid additional parameters effects on the fluid-particles pH value. Fig. 2 demonstrates the schematic procedure of the two-step nanofluids preparation.

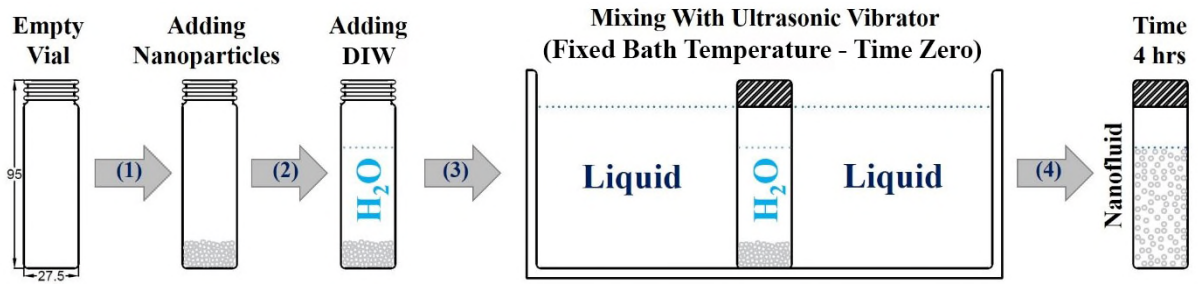

Fig. 2. Schematic procedure for the two-step nanofluids preparation.

Correlations development and validation. The pH value of the basefluid (pH_{bf}) was first measured for three times and averaged, at a temperature range of 10°C to 60°C with an increment of 5°C, as these values reflect the behaviour of the nanofluids with zero nanoparticle concentration. The measurements were then plotted and fitted with a suitable trendline relation in order to obtain the best fit equation, which is valid in the range of $10°C \leq T \leq 60°C$. Next, the average pH values of each material employed to form the nanofluids, of 0.1, 0.5, and 1.0 vol%, were plotted after measuring them at different controlled production temperature, while fixing a single parameter (i.e. sonication bath temperature or particles concentration). The plotted data were then fitted with a trendline relation to acquire their equations and nondimensionalised using a reference temperature (T_0) and a reference basefluid pH value (pH_{bf0}), which were selected to be 25°C and 7, respectively. This was done to have the correlations independent of any units using the surrounding temperature condition. Afterwards, the temperature dependant correlation and the particle concentration correlation were combined together and their regression coefficients were taking as unknown variables. An Excel 2016 data analysis tool was used to determine the new correlation regression coefficient variables and the validation of the proposed correlation was performed by comparing it with the 0.3 and 0.7 vol% as-fabricated nanofluids measured pH values.

Results and discussion

X-ray diffraction analysis and nanoparticles density measurement. The XRD pattern of the as-received SS 316L is shown in Fig. 3(a). It can be notice that only ferrite (BCC) and austenite (FCC) peaks are shown in the plot which indicates that the microstructure is solely composed of these two phases. The crystallite sizes obtained from the strongest Bragg's peaks of the austenite (111) and ferrite (110) phases are about 47 nm and 44 nm, respectively. Figure

3(b) demonstrates the diffraction pattern of the as-received Al NPs. The peaks observed from the analysis shows some oxidation in the Al sample, practically at angles 2θ = 20.46°, 40.80°, and 48.82° which are indexed as (020), (041), and (042), subsequently. Crystallite sizes found at the highest peaks of Al (111) and α-Al_2O_3 (042) are about 50 nm and 91 nm, respectively. Figure 3(c) of the as-received Cu_2O nanopowder pattern shows the present of Cu and CuO peaks, which is normal, since the Cu_2O NPs are very unstable and when exposed to the outer air the material is likely to oxidize to CuO, or return back to Cu. This kind of behaviour was also stated by the manufacturer [49]. Highest peaks of Cu_2O (111), Cu_2O (200), Cu_2O (220), and Cu (111) showed crystallite sizes of 20 nm, 15 nm, 13 nm, and 75 nm, respectively.

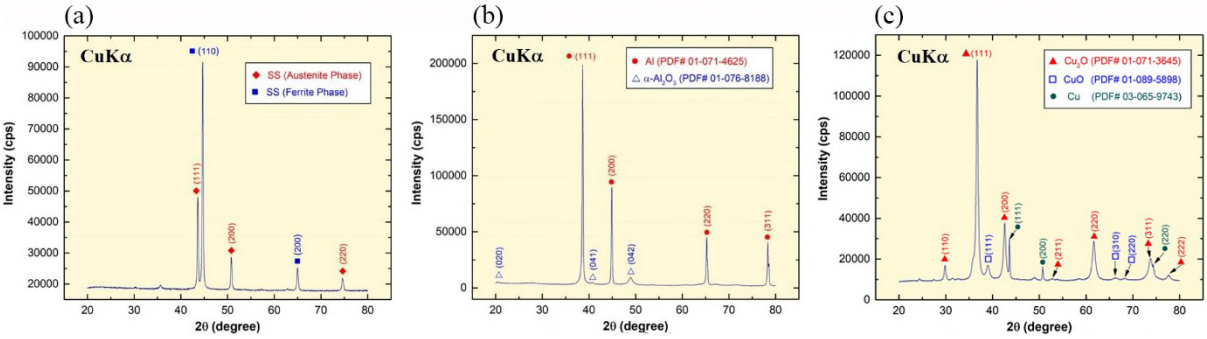

Fig. 3. X-ray diffraction patterns of: (a) Stainless steel 316L NPs, (b) Aluminium NPs, and (c) Copper(I) oxide NPs.

It is worth noting that all crystallite sizes (D_{hkl}) were obtained using the Scherrer formula (Eq. 1), which is commonly used by many researchers [50-53].

$$D_{hkl} = \frac{F\lambda}{\beta_{hkl} cos\theta_{hkl}} \quad (1)$$

Where F represents a constant value equal to 0.9, λ illustrates the wavelength of the CuKα X-ray radiation source and is equal to 0.15405 nm, β_{hkl} demonstrates the full width at half the maximum of the (hkl) diffraction peak, and θ_{hkl} represents the Bragg angle at (hkl) peak.

Density of the as-received SS 316L, Al, and Cu_2O NPs, based on the volume and mass, are shown in Table 2 along with their standard deviation (SD).

Table 2. The as-received nanoparticles densities.

Nanoparticle type	Mass (g)	Sample volume (cm^3)	Density (g/cm^3)	SD × 10^{-2}

Stainless steel 316L	0.2	0.033	6.02	0.18
Aluminium	0.2	0.621	3.22	0.81
Copper(I) oxide	0.2	0.566	3.53	0.14

These density (ρ) values were employed in the mixing theory (Eq. 2) [54], which is widely used and agreed upon by many researchers [16], to calculate the amount of NPs required for the preparation of the nanofluids of selected vol%, where V_{np}, V_{bf}, and m are the NPs volume, basefluid volume, and mass, respectively.

$$vol\% = \frac{V_{np}}{V_{np} + V_{bf}} = \frac{\left(\frac{m}{\rho}\right)_{np}}{\left(\frac{m}{\rho}\right)_{np} + \left(\frac{m}{\rho}\right)_{bf}} \quad (2)$$

Basefluid pH variation with temperature. In this study, DIW was used as the basefluid for preparing the different types of nanofluids. Thus, the pH value of DIW was measured first at a temperature range of 10°C to 60°C, in order to reflect the nanofluids pH values when the concentration of NPs is equal to zero. Figure 4(a) shows the DIW averaged pH value measurements results at different point of temperature, where a monotonic variation in pH with temperature is observed. The highest variation in the pH measurements, within one temperature point, was ±0.05 at 10ºC and 60ºC, and the lowest was ±0.02 at 20ºC to 35ºC. It is important to note that, although the pH value of DIW, of pH 7 at 25ºC, is increasing/decreasing with the change in liquid temperature, the fluid is still considered to be neutral, but only at that point of temperature. This is because, theoretically, rising/lowering the temperature of DIW above/below 25ºC would result in increasing/decreasing the amount of free hydrogen ions and hydroxide ions equally, thus the variation seen in pH value is due to the change in the ionic product constant of water (K_w) [55]. A 3rd order polynomial relation fits the data well and the equation obtained from it (Eq. 3) is valid in the range of 10°C ≤ T ≤ 60°C.

$$pH_{bf} = a_0 + a_1 T + a_2 T^2 + a_3 T^3; \quad (3)$$

With $R^2 = 0.993$

Where the regression constants a_0, a_1, a_2, and a_3 are equal to 7.56, -0.027, 1.86×10^{-4}, and -3.22×10^{-7}, respectively.

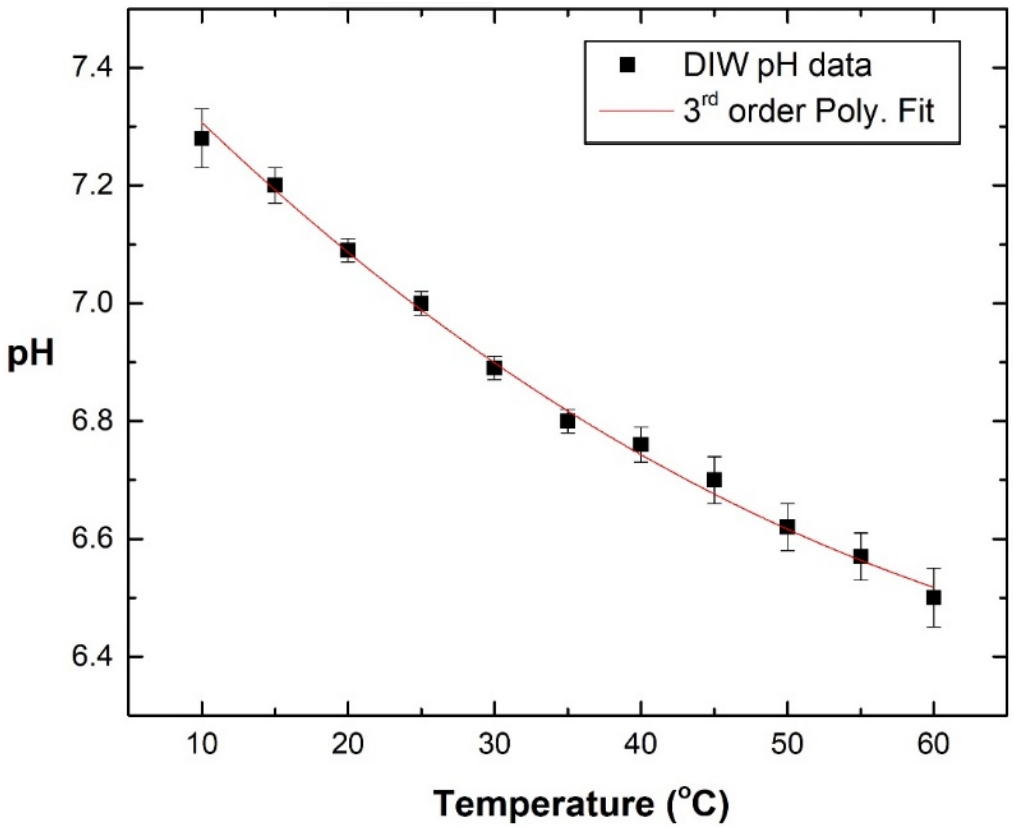

Fig. 4. Measured deionised water pH value at a temperature range from 10ºC to 60ºC.

Nanofluids pH variation. The pH value of SS 316L/DIW, Al_2O_3/DIW, and Cu_2O/DIW nanofluids for three concentrations, namely, 0.1, 0.5, and 1.0 vol% is presented in terms of sonication bath temperature variation (Fig. 5(a-c)) and change in NPs volume percentage (Fig. 6(a-c)). The maximum deviation in the three pH measurements for all three nanofluids, at a single point of temperature, was seen to be ±0.04. Several distinct characteristics of the nanofluids are observed from the plots. Similar to the basefluid behaviour (Fig. 4), the nanofluids pH value tends to decrease with the increase in fabrication temperature. For example, Fig. 5(a) shows a reduction of 4.40, 4.68, and 7.84% in the measured pH values of the 0.1. 0.5, and 1.0 vol% SS 316L nanofluids at a temperature of 60°C compared with their pH values at 10°C. In addition, it was further noticed that the increase in NPs concentration caused the fluid pH value to rise from its initial basefluid state. This kind of outcome is expected, since the added NPs to the basefluid tend to attract the free hydrogen ions within the as-prepared DIW, thus keeping the liquid with higher amount of free hydroxide ions. Hence, the pH_{nf} is predicted to be higher than the pH_{bf} at each preparation temperature.

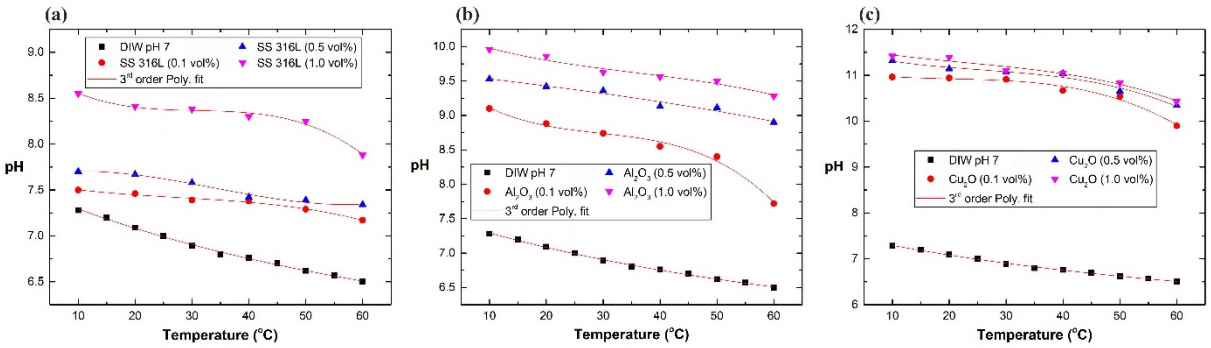

Fig. 5. Nanofluids, of 0.1, 0.5, and 1.0 vol%, pH variation with temperature for: (a) SS 316L/DIW, (b) Al_2O_3/DIW, and (c) Cu_2O/DIW.

Depending on the NPs material used, the nanofluid pH value can either be strongly influenced by the NPs concentration (e.g. SS 316L/DIW and Al_2O_3/DIW), or fixed fabrication temperature (e.g. Cu_2O/DIW). For further illustration, analysing the NPs volumetric concentration and controlled production temperature effect on the pH value of Al_2O_3/DIW nanofluids (Fig. 5(b) and 6(b)) showed that the average change in pH obtained from increasing the concentration alone across the examined temperature range was 11.13%, while increasing the production temperature for each fixed concentration had an average pH variation of 9.53%.

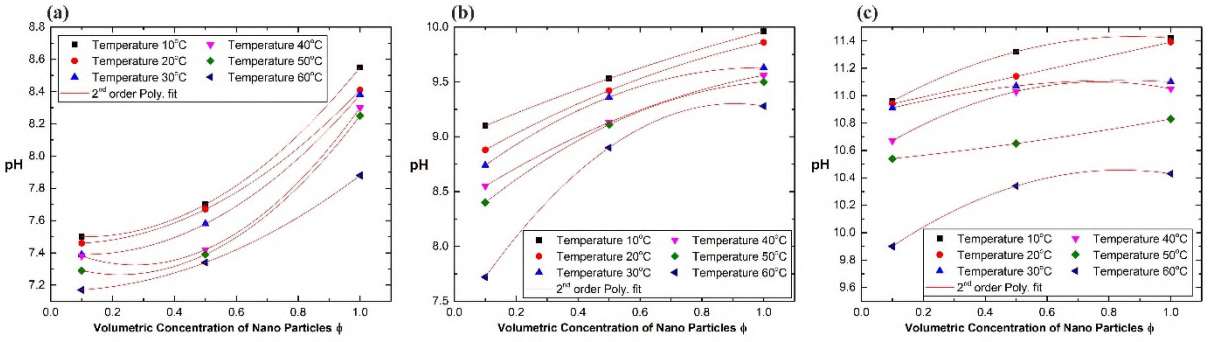

Fig. 6. Nanofluids, of 0.1, 0.5, and 1.0 vol%, pH variation with concentration for: (a) SS 316L/DIW, (b) Al_2O_3/DIW, and (c) Cu_2O/DIW.

In addition, it can be seen that all three types of nanofluids pH data, at a specific concentration, follows a 3rd order polynomial relation fit which can be expressed by Eq. 4 along with the regression constants shown in Table 3.

$$pH_{nf} = b_0 + b_1 \mathrm{T} + b_2 T^2 + b_3 T^3 \quad (4)$$

Furthermore, from the data in Fig. 6, at each as-prepared fluid fabrication temperature, the variation in pH value in respect of NPs volume percentage is seen to cohabit a 2nd order polynomial relation, for all three types of nanofluids, which can be expressed as:

$$pH_{nf} = c_0 + c_1\phi + c_2\phi^2 \quad (5)$$

With $R^2 = 1$

Equations 4 and 5 are valid in the range of 10°C ≤ T ≤ 60°C, and 0.1 vol% ≤ φ ≤ 1.0 vol% with the regression constants of Eq. 5 (i.e. c_0, c_1, and c_2) are tabulated in Table 4.

Table 3. Regression coefficients of Eq. 4 for SS 316L, Al_2O_3/DIW, and Cu_2O/DIW nanofluids.

Regression constants	SS 316L/DIW			Al_2O_3/DIW			Cu_2O/DIW		
	0.1 vol%	0.5 vol%	1.0 vol%	0.1 vol%	0.5 vol%	1.0 vol%	0.1 vol%	0.5 vol%	1.0 vol%
b_0	7.60	7.63	8.93	9.68	9.63	10.24	11.10	11.56	11.64
b_1	-0.013	0.014	-0.052	-0.077	-0.01	-0.032	-0.021	-0.033	-0.024
b_2	3.226×10^{-4}	-7.528×10^{-4}	1.64×10^{-3}	0.0023	-2.381×10^{-6}	5.976×10^{-4}	8.722×10^{-4}	9.361×10^{-4}	5.266×10^{-4}
b_3	-3.889×10^{-6}	7.407×10^{-6}	-1.769×10^{-5}	-2.574×10^{-5}	-5.556×10^{-7}	-5.556×10^{-6}	-1.426×10^{-5}	-1.213×10^{-5}	-7.685×10^{-6}
R^2	0.974	0.959	0.970	0.978	0.921	0.932	0.955	0.950	0.941

Table 4. Regression coefficients of Eq. 5 for SS 316L, Al_2O_3/DIW, and Cu_2O/DIW nanofluids.

Temperature (°C)	SS 316L/DIW			Al_2O_3/DIW			Cu_2O/DIW		
	c_0	c_1	c_2	c_0	c_1	c_2	c_0	c_1	c_2
10	7.52	-0.300	1.333	8.98	1.218	-0.239	10.83	1.367	-0.778
20	7.46	-0.112	1.061	8.72	1.663	-0.522	10.89	0.5	4.428×10^{-15}
30	7.40	-0.275	1.250	8.53	2.223	-1.122	10.85	0.627	-0.378
40	7.46	-1.007	1.844	8.37	1.843	-0.656	10.53	1.473	-0.956
50	7.35	-0.730	1.633	8.17	2.438	-1.106	10.52	0.218	0.094
60	7.16	-0.012	0.728	7.30	4.410	-2.433	9.74	1.713	-1.022

Correlation development. From analysing the experimental results of Fig. 5 and Fig. 6, it was found that the pH value of each type of nanofluid examined depends on the volumetric concentration of the NPs used and the temperature of suspension fabrication. In order to establish a joint link between the two parameters (i.e. T and ϕ) and the nanofluid pH value, an analysis of the variation of these parameters independently was carried out. Having the correlation independent of any units, the pH_{nf} was nondimensionalised by that of the basefluid, at room temperature conditions, using the parameters pH_{bf0} and T_0 values.

Influence of temperature. The pH values of SS 316L/DIW, Al_2O_3/DIW, and Cu_2O/DIW nanofluids in Fig. 5 were nondimensionalised using the value of pH_{bf0} then plotted in contrast to the nondimensionalised temperature $(\frac{T}{T_0})$, for each of the three nanoparticle concentrations. It can be observed from Fig. 7 that the pH ratio $(\frac{pH_{nf}}{pH_{bf0}})$ against $(\frac{T}{T_0})$ corresponds to a 3rd order polynomial relation. Thus, the correlation for $(\frac{pH_{nf}}{pH_{bf0}})$ as a function of $(\frac{T}{T_0})$ can be best represented as:

$$\frac{pH_{nf}}{pH_{bf0}} = d_0 + d_1(\frac{T}{T_0}) + d_2(\frac{T}{T_0})^2 + d_3(\frac{T}{T_0})^3 \quad (6)$$

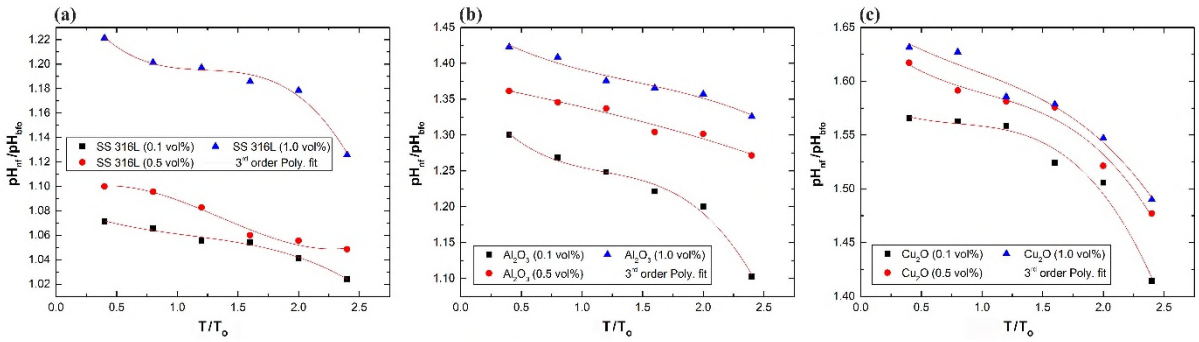

Fig. 7. Nanofluids, of 0.1, 0.5, and 1.0 vol%, nondimensionalised pH variation against $(\frac{T}{T_0})$ for: (a) SS 316L/DIW, (b) Al_2O_3/DIW, and (c) Cu_2O/DIW.

Influence of concentration. From Fig. 6 and Eq. 5, it was demonstrated that the variation in pH_{nf} as a function of ϕ followed a 2nd order polynomial relation at a fixed fabrication temperature. This was examined for all three types of nanofluids that were produced from a controlled sonication bath temperature that ranged from 10°C to 60°C. Due to the nature of Eq. 5, the appropriate nondimensionalisation representation of the correlation can be shown as following:

$$\frac{pH_{nf}}{pH_{bf0}} = e_0 + e_1\phi + e_2\phi^2 \quad (7)$$

Proposed correlation. From the previous two analysis of the influence of each parameter, it was found that a general pH_{nf} correlation can be illustrated by combining Eq. 6 and Eq. 7 in the following format:

$$\frac{pH_{nf}}{pH_{bf0}} = \left[d_o + d_1(\frac{T}{T_0}) + d_2(\frac{T}{T_0})^2 + d_3(\frac{T}{T_0})^3\right].[e_0 + e_1\phi + e_2\phi^2] \quad (8)$$

Equation 8 was then extended to Eq. 9 because of the infinite number of solutions that can be obtained at the current state to the regression coefficients.

$$\frac{pH_{nf}}{pH_{bf0}} = X_0 + X_1(\frac{T}{T_0}) + X_2(\frac{T}{T_0})^2 + X_3(\frac{T}{T_0})^3 + X_4\phi + X_5\phi(\frac{T}{T_0}) + X_6\phi(\frac{T}{T_0})^2 +$$
$$X_7\phi(\frac{T}{T_0})^3 + X_8\phi^2 + X_9\phi^2(\frac{T}{T_0}) + X_{10}\phi^2(\frac{T}{T_0})^2 + X_{11}\phi^2(\frac{T}{T_0})^3 \quad (9)$$

Where the correspondence of the new regression coefficients (i.e. X_0 to X_{11}) are shown in Table 5.

Table 5. Regression coefficients of Eq. 9 and their correspondence.

Regression coefficient	Representation	Regression coefficient	Representation	Regression coefficient	Representation
X_0	$d_o.e_0$	X_4	$d_o.e_1$	X_8	$d_o.e_2$
X_1	$d_1.e_0$	X_5	$d_1.e_1$	X_9	$d_1.e_2$
X_2	$d_2.e_0$	X_6	$d_2.e_1$	X_{10}	$d_2.e_2$
X_3	$d_3.e_0$	X_7	$d_3.e_1$	X_{11}	$d_3.e_2$

The Excel 2016 data analysis regression tool was then used to determine the values of the unknown regression coefficients of Eq. 9 for the different types of nanofluids from their nondimensionalised pH_{nf} measured data and $(\frac{T}{T_0})$. Table 6 shows the statistical analysis tabulation of the regression coefficients, where Eq. 9 with the coefficients of Table 6 has a range of validity of 10°C ≤ T ≤ 60°C, and 0.1 vol% ≤ φ ≤ 1.0 vol%.

Table 6. Regression coefficients of Eq. 9 values for different as-fabricated nanofluids.

Regression constant	SS 316L/DIW	Al_2O_3/DIW	Cu_2O/DIW
X_0	1.104	1.395	1.562
X_1	-0.107	-0.376	-0.053
X_2	0.090	0.289	0.072
X_3	-0.025	-0.081	-0.033
X_4	-0.227	-0.144	0.255
X_5	0.703	1.099	-0.229
X_6	-0.685	-0.922	0.073
X_7	0.180	0.249	0.007
X_8	0.397	0.212	-0.154
X_9	-0.781	-0.837	0.197
X_{10}	0.741	0.686	-0.097
X_{11}	-0.195	-0.181	0.009
R^2	0.995	0.985	0.953
Maximum deviation	-0.90%	-1.24%	+0.95%
Average deviation	0.28%	0.50%	0.38%

Validation of the new correlation. In order to validate the newly developed correlation, the pH of the as-prepared 0.3 and 0.7 vol% nanofluids of different fixed fabrication temperatures were compared with the proposed correlation in terms of experimental measurement against

theoretical computation as demonstrated in Fig. 8. The central line in Fig. 8(a-b) represents a perfect match between the new correlation values and the experimental data. It can be notice that there exists some level of deviation between the measured data and the correlation prediction, especially with the measured data of SS 316L/DIW nanofluid. Nevertheless, the correlation shows very good estimation towards the pH_{nf} for all three types of nanofluids, where the highest prediction error was shown to be -8.09% (at T = 40°C and φ = 0.7 vol%) for SS 316L/DIW, +5.08% (at T = 60°C and φ = 0.7 vol%) for Al_2O_3/DIW, and +2.31% (at T = 60°C and φ = 0.7 vol%) for Cu_2O/DIW. The average error of the newly proposed correlation, for the 0.1-1.0 vol% SS 316L/DIW, Al_2O_3/DIW, and Cu_2O/DIW samples, was found to be 2.18%, 0.92%, and 0.63%, respectively. Given a specific controlled sonication bath temperature and NPs concentration, the correlation of Eq. 9 insures at least 91% confidence that the value will be between the upper and lower prediction error limits of the curve-fit range. Such level of error is acceptable for many industrial applications, since the highest deviation from the actual pH_{nf} measurement would be within a value of ±0.57 (i.e. less than 1).

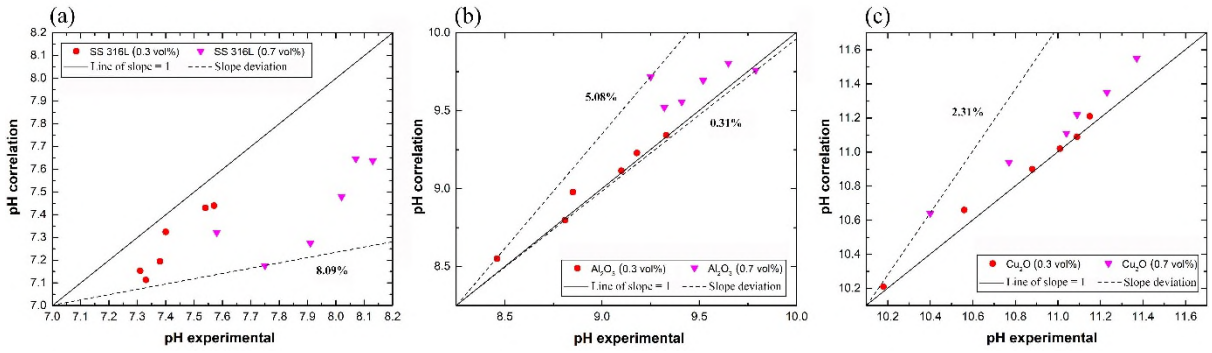

Fig. 8. Comparison between the new correlation prediction (Eq. 9) and the measured pH of: (a) SS 316L/DIW, (b) Al_2O_3/DIW, and (c) Cu_2O/DIW.

Summary

Measurements of the pH value of three types of nanofluids, namely, SS 316L/DIW, Al_2O_3/DIW, and Cu_2O/DIW were performed in order to develop a general correlation that can predict the pH_{nf} value, within the conducted experiments range, from the liquid production temperature and nanoparticle volumetric concentration. All three types of nanofluids were fabricated using a controlled sonication bath temperature two-step approach, with 0.1 to 1.0 vol% of NPs. The following conclusions are drawn:

- The experimental findings have indicated that, increasing the NPs concentration in the basefluid had an alkaline effect, while rising the temperature caused the nanofluid to be more acidic. Such behaviours are expected to be a result of: 1- the NPs attraction of free hydrogen ions within the basefluid, and 2- the increase in the amount of ions been freed from their water molecules caused by the rise in fluid temperature.
- In addition, depending on the nanoparticle material, the pH_{nf} can be strongly influenced by either the controlled sonication bath temperature, as in the case of Cu_2O/DIW, or the changes in nanofluid particle concentration (e.g. SS 316L/DIW, and Al_2O_3/DIW). For instant, by analysing the pH value of Al_2O_3/DIW for the two aforementioned parameters, the average change in pH_{nf} due to increasing the particles volumetric concentration alone over the fixed bath temperatures have shown to be 11.13%, whereas varying the processing controlled temperatures for each volumetric concentration has resulted in a 9.53% average change in pH.
- Using the experimental data, a new pH_{nf} correlation was developed as a function of fabrication bath temperature and NPs volume concentration to estimate the pH value of the three previous types of nanofluids. The proposed correlation has illustrated a high prediction capability, where its average error for SS 316L/DIW, Al_2O_3/DIW, and Cu_2O/DIW have shown to be 2.18%, 0.92%, and 0.63%, respectively.

Nevertheless, it should be acknowledged that, due to the variation in nanofluid dispersant methods and their NPs crystal structures, the presented correlation are very helpful and reliable for applications that uses nanofluids fabricated similarly to the conducted study approach and parametric range. These correlations will be advanced for additional parameters such as NPs average size, shape, and the existence of surfactants.

Acknowledgements

The authors of this manuscript wish to acknowledge the help and support provided by their institutes for conducting this research work.

References

[1] S.U.S. Choi, J.A. Eastman, Enhancing thermal conductivity of fluids with nanoparticles, ; Argonne National Lab., IL (United States), 1995.

[2] P. Keblinski, J.A. Eastman, D.G. Cahill, Nanofluids for thermal transport, Materials Today, 8 (2005) 36-44.

[3] C. Anushree, J. Philip, Assessment of long term stability of aqueous nanofluids using different experimental techniques, Journal of Molecular Liquids, 222 (2016) 350-358.

[4] S.U. Ilyas, R. Pendyala, A.S. Shuib, N. Marneni, A review on the viscous and thermal transport properties of nanofluids, in: International Conference on Process Engineering and Advanced Materials, ICPEAM 2012, Trans Tech Publications Ltd, Kuala Lumpur, 2014, pp. 18-27.

[5] R. Shanthi, S.S. Anandan, V. Ramalingam, HEAT TRANSFER ENHANCEMENT USING NANOFLUIDS An Overview, Therm. Sci., 16 (2012) 423-444.

[6] D.S. Wen, G.P. Lin, S. Vafaei, K. Zhang, Review of nanofluids for heat transfer applications, Particuology, 7 (2009) 141-150.

[7] L. Vekas, D. Bica, M.V. Avdeev, Magnetic nanoparticles and concentrated magnetic nanofluids: Synthesis, properties and some applications, China Particuology, 5 (2007) 43-49.

[8] K.S. Reddy, N.R. Kamnapure, S. Srivastava, Nanofluid and nanocomposite applications in solar energy conversion systems for performance enhancement: a review, Int. J. Low Carbon Technol., 12 (2017) 1-23.

[9] M. Sheikholeslami, D.D. Ganji, Chapter 1 - Application of Nanofluids, in: M. Sheikholeslami, D.D. Ganji (Eds.) Applications of Semi Analytical Methods for Nanofluid Flow and Heat Transfer, Elsevier, 2018, pp. 1-44.

[10] D. Mansoury, I.D. Faramarz, A. Kiani, A.J. Chamkha, M. Sharifpur, Heat transfer and flow characteristics of Al2O3/water nanofluid in various heat exchangers: Experiments on counter flow, Heat Transfer Eng, (2018) 1-36.

[11] A.J. Chamkha, M. Molana, A. Rahnama, F. Ghadami, On the nanofluids applications in microchannels: A comprehensive review, Powder Technol., 332 (2018) 287-322.

[12] S.U. Ilyas, R. Pendyala, N. Marneni, Stability and Agglomeration of Alumina Nanoparticles in Ethanol-Water Mixtures, in: M.A. Bustam, L.K. Keong, Z. Man, A.A. Hassankiadeh, Y.Y. Fong (Eds.) 4th International Conference on Process Engineering and Advanced Materials, ICPEAM 2016, Elsevier Ltd, 2016, pp. 290-297.

[13] S.U. Ilyas, R. Pendyala, N. Marneni, Preparation, Sedimentation, and Agglomeration of Nanofluids, Chemical Engineering & Technology, 37 (2014) 2011-2021.

[14] S. Mukherjee, P.C. Mishra, P. Chaudhuri, Stability of Heat Transfer Nanofluids – A Review, ChemBioEng Reviews, 5 (2018) 312-333.

[15] M.K. Bushehri, A. Mohebbi, H.H. Rafsanjani, Prediction of Thermal Conductivity and Viscosity of Nanofluids by Molecular Dynamics Simulation, J. Eng. Thermophys., 25 (2016) 389-400.

[16] N. Ali, J.A. Teixeira, A. Addali, A Review on Nanofluids: Fabrication, Stability, and Thermophysical Properties, J. Nanomater., 2018 (2018) 33.

[17] J. Hong, D. Kim, Effects of aggregation on the thermal conductivity of alumina/water nanofluids, Thermochim Acta, 542 (2012) 28-32.

[18] O. Arthur, M.A. Karim, An investigation into the thermophysical and rheological properties of nanofluids for solar thermal applications, Renewable & Sustainable Energy Reviews, 55 (2016) 739-755.

[19] K.S. Suganthi, K.S. Rajan, Metal oxide nanofluids: Review of formulation, thermo-physical properties, mechanisms, and heat transfer performance, Renewable & Sustainable Energy Reviews, 76 (2017) 226-255.

[20] I.M. Mahbubul, E.B. Elcioglu, R. Saidur, M.A. Amalina, Optimization of ultrasonication period for better dispersion and stability of TiO2-water nanofluid, Ultrason Sonochem, 37 (2017) 360-367.

[21] P.K. Das, A review based on the effect and mechanism of thermal conductivity of normal nanofluids and hybrid nanofluids, Journal of Molecular Liquids, 240 (2017) 420-446.

[22] X.F. Peng, X.L. Yu, L.F. Xia, X. Zhong, Influence factors on suspension stability of nanofluids, Zhejiang Daxue Xuebao (Gongxue Ban), 41 (2007) 577-580.

[23] R. Choudhary, D. Khurana, A. Kumar, S. Subudhi, Stability analysis of Al2O3/water nanofluids, J. Exp. Nanosci., 12 (2017) 140-151.

[24] H. Zhu, C. Zhang, Y. Tang, J. Wang, B. Ren, Y. Yin, Preparation and thermal conductivity of suspensions of graphite nanoparticles, 2007.

[25] X. Li, D. Zhu, X. Wang, Evaluation on dispersion behavior of the aqueous copper nano-suspensions, J Colloid Interface Sci, 310 (2007) 456-463.

[26] E.B. Haghighi, N. Nikkam, M. Saleemi, M. Behi, S.A. Mirmohammadi, H. Poth, R. Khodabandeh, M.S. Toprak, M. Muhammed, B. Palm, Shelf stability of nanofluids and its effect on thermal conductivity and viscosity, Meas. Sci. Technol., 24 (2013).

[27] S. Askari, H. Koolivand, M. Pourkhalil, R. Lotfi, A. Rashidi, Investigation of Fe3O4/Graphene nanohybrid heat transfer properties: Experimental approach, Int. Commun. Heat Mass Transf., 87 (2017) 30-39.

[28] M. Mohammadi, M. Dadvar, B. Dabir, TiO2/SiO2 nanofluids as novel inhibitors for the stability of asphaltene particles in crude oil: Mechanistic understanding, screening, modeling, and optimization, Journal of Molecular Liquids, 238 (2017) 326-340.

[29] K.Y. Leong, Z.A. Najwa, K.Z.K. Ahmad, H.C. Ong, Investigation on Stability and Optical Properties of Titanium Dioxide and Aluminum Oxide Water-Based Nanofluids, Int J Thermophys, 38 (2017).

[30] P.C.M. Kumar, M. Muruganandam, Stability Analysis of Heat Transfer MWCNT with Different Base Fluids, J. Appl. Fluid Mech., 10 (2017) 51-59.

[31] A. Menbari, A.A. Alemrajabi, Y. Ghayeb, Investigation on the stability, viscosity and extinction coefficient of CuO-Al2O3/Water binary mixture nanofluid, Exp. Therm. Fluid Sci., 74 (2016) 122-129.

[32] Y. Hwang, J.K. Lee, J.K. Lee, Y.M. Jeong, S.I. Cheong, Y.C. Ahn, S.H. Kim, Production and dispersion stability of nanoparticles in nanofluids, Powder Technol., 186 (2008) 145-153.

[33] W. Yu, H.Q. Xie, A Review on Nanofluids: Preparation, Stability Mechanisms, and Applications, J. Nanomater., 2012 (2012).

[34] X.J. Wang, D.S. Zhu, S. Yang, Investigation of pH and SDBS on enhancement of thermal conductivity in nanofluids, Chem. Phys. Lett., 470 (2009) 107-111.

[35] X.F. Li, D.S. Zhu, X.J. Wang, N. Wang, J.W. Gao, H. Li, Thermal conductivity enhancement dependent pH and chemical surfactant for Cu-H2O nanofluids, Thermochim Acta, 469 (2008) 98-103.

[36] S. Witharana, I. Palabiyik, Z. Musina, Y.L. Ding, Stability of glycol nanofluids - The theory and experiment, Powder Technol., 239 (2013) 72-77.

[37] J. Lee, K. Han, J. Koo, A novel method to evaluate dispersion stability of nanofluids, Int. J. Heat Mass Transf., 70 (2014) 421-429.

[38] D.S. Zhu, X.F. Li, N. Wang, X.J. Wang, J.W. Gao, H. Li, Dispersion behavior and thermal conductivity characteristics of Al2O3-H2O nanofluids, Curr. Appl. Phys., 9 (2009) 131-139.

[39] M. Modak, S.S. Chougule, S.K. Sahu, An Experimental Investigation on Heat Transfer Characteristics of Hot Surface by Using CuO-Water Nanofluids in Circular Jet Impingement Cooling, Journal of Heat Transfer-Transactions of the Asme, 140 (2018).

[40] S. Manjula, S.M. Kumar, A.M. Raichur, G.M. Madhu, R. Suresh, M.A.L.A. Raj, A sedimentation study to optimize the dispersion of alumina nanoparticles in water, Cerâmica, 51 (2005) 121-127.

[41] S. Witharana, C. Hodges, D. Xu, X.J. Lai, Y.L. Ding, Aggregation and settling in aqueous polydisperse alumina nanoparticle suspensions, J. Nanopart. Res., 14 (2012).

[42] D. Lee, J.W. Kim, B.G. Kim, A new parameter to control heat transport in nanofluids: surface charge state of the particle in suspension, J Phys Chem B, 110 (2006) 4323-4328.

[43] Y.Y. Song, H.K.D.H. Bhadeshia, D.W. Suh, Stability of stainless-steel nanoparticle and water mixtures, Powder Technol., 272 (2015) 34-44.

[44] N. Ali, J.A. Teixeira, A. Addali, F. Al-Zubi, E. Shaban, I. Behbehani, The effect of aluminium nanocoating and water pH value on the wettability behavior of an aluminium surface, Applied Surface Science, 443 (2018) 24-30.

[45] N. Ali, J.A. Teixeira, A. Addali, M. Saeed, F. Al-Zubi, A. Sedaghat, H. Bahzad, Deposition of Stainless Steel Thin Films: An Electron Beam Physical Vapour Deposition Approach, Materials, 12 (2019) 571.

[46] S. Nanomaterials, Stainless Steel Nanoparticles/ Nanopowder, in, https://ssnano.com/inc/sdetail/stainless_steel_nanoparticles/2760, 2017.

[47] Hach, User Manual - General use pH probe: Models PHC20101, PHC20103 (DOC022.53.80197), in, Hach Company, https://www.hach.com/asset-get.download.jsa?id=8027841104, 2013.

[48] Hach, Application note - Temperature Compensation With pH Measurement in, Hach Company, https://www.hach.com/asset-get.download.jsa?id=17525673904, 2013.

[49] I. US Research Nanomaterials, Copper(I) Oxide (Cuprous Oxide) Nanopowder / Cu2O Nanoparticles, in, 2017.

[50] X.W. Ai, J.X. Lin, Y.F. Chang, L.Q. Zhou, X.M. Zhang, G.W. Qin, Phase modification of copper phthalocyanine semiconductor by converting powder to thin film, Applied Surface Science, 428 (2018) 788-792.

[51] P.V. Raleaooa, A. Roodt, G.G. Mhlongo, D.E. Motaung, O.M. Ntwaeaborwa, Analysis of the structure, particle morphology and photoluminescent properties of ZnS:Mn2+ nanoparticulate phosphors, Optik, 153 (2018) 31-42.

[52] M. Rabiee, H. Mirzadeh, A. Ataie, Processing of Cu-Fe and Cu-Fe-SiC nanocomposites by mechanical alloying, Adv Powder Technol, 28 (2017) 1882-1887.

[53] S. Minaei, M. Haghighi, N. Jodeiri, H. Ajamein, M. Abdollahifar, Urea-nitrates combustion preparation of CeO2-promoted CuO/ZnO/Al2O3 nanocatalyst for fuel cell grade hydrogen production via methanol steam reforming, Adv Powder Technol, 28 (2017) 842-853.

[54] B.C. Pak, Y.I. Cho, Hydrodynamic and heat transfer study of dispersed fluids with submicron metallic oxide particles, Exp. Heat Transf., 11 (1998) 151-170.

[55] W.L. Marshall, E.U. Franck, Ion product of water substance, 0–1000 °C, 1–10,000 bars New International Formulation and its background, J. Phys. Chem. Ref. Data, 10 (1981) 295-304.